

7th International Conference on Silicon Photovoltaics, SiliconPV 2017

Distributed series resistance in a one-dimensional two-diode model revisited

Jan-Martin Wagner^{a,*}, Sven Rißland^b, Andreas Schütt^c, Jürgen Carstensen^a,
Rainer Adelung^a

^aUniversity of Kiel, Faculty of Engineering, Chair of Functional Nano-Materials, Kaiserstr. 2, 24143 Kiel, Germany

^bFormerly with Max Planck Institute of Microstructure Physics, former Department 2, Weinberg 2, 06120 Halle (Saale), Germany

^cCELLOscan GbR, Gravelottestr. 5, 24116 Kiel, Germany

Abstract

The lumped series resistance R_s of large-area silicon solar cells, obtained from current–voltage ($I-U$) data according to the two-light-level method, varies along the $I-U$ characteristic. Such a variation can most simply be described by the linear-response series resistance model (LR- R_s), recently developed in connection with luminescence imaging. Here, independently obtained experimental data are used to test the applicability of the LR- R_s model to R_s data based on $I-U$ characteristics. After subtracting a non-distributed part from the measured R_s data, the inverse of the remaining distributed part shows a scaling proportional to the inverse of the bias-dependent diode resistance; a slope value of 1 is used as predicted by the LR- R_s model applied to a laterally one-dimensional geometry. The same experimental data have previously been interpreted based on a mathematically rather complicated model published already many years ago; just recently it was found that in some cases this model may lead to unphysical results. The present LR- R_s model based proper interpretation of the variation of the lumped series resistance along the $I-U$ characteristic leads to a roughly half-by-half splitting between the distributed and the non-distributed part of R_s . This share has been observed many years for “economically reasonable” solar cells investigated by the CELLO technique. The successful usage of the LR- R_s model for $I-U$ based R_s data is a strong hint that its underlying physical concepts are of general validity.

© 2017 The Authors. Published by Elsevier Ltd.

Peer review by the scientific conference committee of SiliconPV 2017 under responsibility of PSE AG.

Keywords: standard equivalent circuit ; current–voltage characteristic ; series resistance ; injection dependence ; one-dimensional solar cell modeling ; linear response theory

* Corresponding author. Tel.: +49-431-880-6181; fax: +49-431-880-6124.
E-mail address: jwa@tf.uni-kiel.de

1. Introduction

The conventional two-diode model is the standard description for the current–voltage (I – U) characteristic of a silicon solar cell. This equivalent circuit model contains the following parameters: photocurrent density (J_{ph}), saturation current density and ideality factor of first and second diode (J_{01}, J_{02} and n_1, n_2 , respectively), lumped series resistance (R_s), and global parallel (shunt) resistance (R_p). Experimentally, however, it is found that the series resistance of large-area silicon solar cells changes along the I – U characteristic. This effect is due to R_s partly being distributed; it is known since many years (cf., e.g., [1–6]). Since in the conventional two-diode model R_s is constant, this model does not hold correctly at high injection levels. There are some theoretical works in the literature describing this variation of R_s along the I – U characteristic (cf., e.g., [7–10]), most of them making use of quite intricate mathematics. However, only recently it was shown that in cases of practical relevance this variation can be described quite simply [6] and that one of the previous theoretical approaches [9] in some cases may lead to unphysical results [6] (see also the discussion below). In previous works [11, 12], measured I – U data were interpreted according to the latter series resistance theory [9], so it is not clear whether their R_s description is accurate. Here, we use the previously published I – U based series resistance data [11, 12] to test the applicability of the newly proposed linear-response series resistance (LR- R_s) model that so far is well confirmed only for luminescence [6] and CELLO measurements [13] (and references therein).

2. Experimental

In the present work, we re-interpret already-measured data, originally published in [11, 12]. Nevertheless, here we give a brief summary about how those data were obtained and how the lumped series resistance was extracted. The measurement of the I – U characteristics was done on a water-cooled measurement chuck, always keeping the cell at 25 °C (even under varying illumination). To that end, the solar cell surface temperature was independently measured by an IR thermometer. Two different multi-crystalline silicon solar cells with full-area Al back surface field have been investigated: cell A is a standard industrial cell of size (156 mm)², whereas cell B is a research lab cell of size (125 mm)²; further specifications can be found in [11, 12]. The cells were sucked on to the chuck by vacuum and were biased by a four-quadrant power supply. A four-probe contact scheme was used including additional sense pins contacting the middle of each front side busbar and one pin sensing the rear side contact. The I – U measurements were made both in the dark as well as under illumination (with light of 850 nm).

From the measured I – U data, the lumped series resistance data (varying along the I – U characteristic) were extracted as described in detail in [11, 12]. Here, we only give a brief summary of this procedure: From the low-voltage part (where R_s can be neglected), the two-diode model parameters were determined for fixed $n_1 = 1$. From a comparison with the measured open-circuit voltage (where R_s is irrelevant), for cell A the value of n_1 was slightly increased to account for an injection-dependent lifetime, and the value of J_{01} was adjusted to match this value of n_1 , altogether reproducing the measured open-circuit voltage [11, 12]; for cell B, n_1 remains unity throughout.

Knowing all the two-diode parameters enables one to calculate the effective diode voltage (in the standard one-diode equivalent circuit) for the illuminated I – U characteristic at all lumped dark diode currents, $U_{\text{D,calc}}(I_{\text{D}})$, and thus to evaluate the lumped series resistance (in m Ω) corresponding to this lumped dark diode current I_{D} according to

$$R_s(I_{\text{D}}) = \frac{U_{\text{ext,dark}}(I_{\text{D}}) - U_{\text{D,calc}}(I_{\text{D}})}{I_{\text{D}}} \quad (1)$$

Since two pairs of I – U data (one directly from the dark characteristic, the other calculated from the two-diode parameters that reproduce the illuminated characteristic) are used for this R_s determination, belonging to the same dark diode current, this method to obtain R_s from the measurements follows the same concept as the two-light-level method for the determination of the series resistance (cf., e.g., [1, 3, 4]). For the application of the LR- R_s model (explained in the following section), the lumped dark diode current (varying over several ampere) is converted to the inverse of the lumped effective diode resistance R_{D} (i.e., the lumped effective diode conductance G_{D}) by

$$\frac{1}{R_D} = G_D = \frac{I_D}{U_{\text{therm}}}, \tag{2}$$

with $U_{\text{therm}} = k_B T / e$. The $R_s(G_D)$ data are shown for cell A in Fig. 1(a), together with curves stemming from the LR- R_s model. For cell B, the corresponding data are shown in Fig. 2(a). The data shown in Figs 1(b) and 2(b), being related to the distributed part of the series resistance only, are described and discussed below (Sects. 3 and 4).

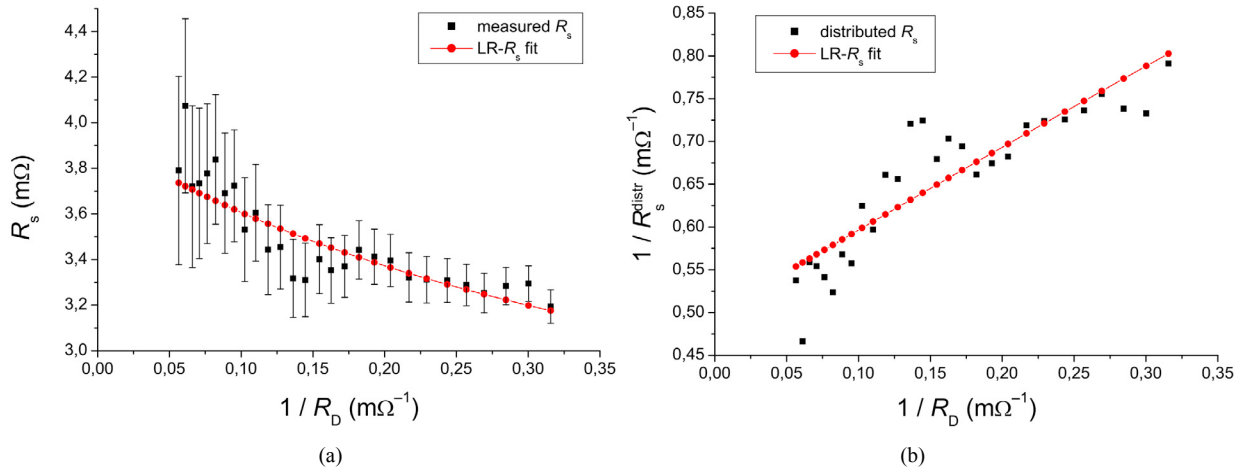


Fig. 1. Series resistance data of cell A (standard industrial Al BSF multi-crystalline silicon solar cell, edge length: 156 mm). (a) Lumped series resistance (black squares: measured data [11, 12], red points: LR- R_s model) versus reciprocal diode resistance. (b) Inverse of the distributed part of the series resistance (black squares: measured data, red points: LR- R_s model) versus inverse of the diode resistance; the LR- R_s model data form a straight line with a slope of $g = 1$ [cf. Eq. (3) below].

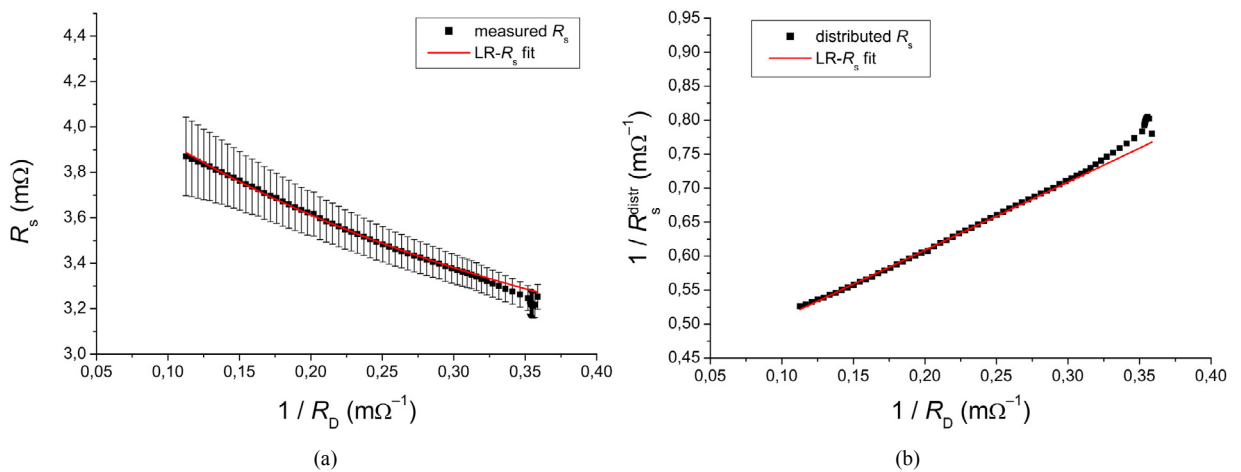


Fig. 2. Series resistance data of cell B (Al BSF multi-crystalline silicon solar cell, edge length: 152 mm). (a) Lumped series resistance (black squares: measured data [12], red curve: LR- R_s model) versus reciprocal diode resistance. (b) Inverse of the distributed part of the series resistance (black squares: measured data, red curve: LR- R_s model) versus inverse of the diode resistance; the LR- R_s model data form a straight line with a slope of $g = 1$ [cf. Eq. (3) below].

3. Modeling

The properties of the LR- R_s model have been described extensively in Ref. [6] (see also references therein) and are briefly reviewed here. In the latter publication, a luminescence imaging approach is used to separately determine the distributed part R_s^{distr} of the total series resistance. (Note that although in [6] luminescence images were used, here the LR- R_s model refers to the *lumped* series resistance.) Motivated by previous CELLO series resistance evaluations [13] (and references therein), the inverse of the distributed part of the lumped series resistance is plotted versus the lumped effective diode conductance $G_D = 1 / R_D$, which is a measure for the overall injection level of the whole solar cell. In this plot one obtains a straight line with a certain slope g . The intersection of this straight line with the ordinate gives the inverse of the average distributed series resistance for infinite diode resistance and is therefore called $R_{s,\infty}^{-1}$. One can therefore express the observed linear relationship as

$$\frac{1}{R_s^{\text{distr}}} = \frac{1}{R_{s,\infty}} + g \frac{1}{R_D}. \quad (3)$$

This distributed part just adds to the non-distributed part, *i.e.* $R_s = R_s^{\text{nondistr}} + R_s^{\text{distr}}$, so the total series resistance is

$$R_s = R_s^{\text{nondistr}} + \frac{1}{1/R_{s,\infty} + g/R_D}. \quad (4)$$

This expression, directly derived from experiment [6], results in a new equivalent circuit, Fig. 3, deviating only slightly from the conventional one but fully including the variation of R_s along the I - U characteristic due to its partly distributed nature. The diode in this equivalent circuit is the first diode of the conventional two-diode model since this diode determines the overall injection level at the voltages where the decrease of the series resistance occurs.

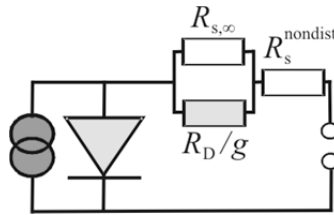


Fig. 3. Equivalent circuit corresponding to the LR- R_s model, Eq. (4), consistent with the variation of the series resistance along the I - U characteristic due to the varying diode resistance R_D (*i.e.*, including the dark-diode-current dependence of the series resistance).

To understand this lumped equivalent circuit from a theoretical point of view, as motivated by the experimental observations noted in [11, 12] also here we consider an effective laterally one-dimensional geometry for the analytical description of the distributed series resistance (from which the lumped properties are derived). The details of the calculation are given in appendix A, but the underlying concept is briefly explained here. The basic steps that are described in the following are the general framework of the theory behind the LR- R_s model; they are always applied, independent of the geometry and dimensionality under investigation (*e.g.*, a 2D model was treated in [14]).

The first basic step of our approach is to consider, for a fixed lumped dark diode current determining the solar cell's working point, the small-signal response of the external voltage to a change in external current, both being deviations from the given working-point values; this explains why our approach is termed linear-response series resistance (LR- R_s) model. Basically, in this small-signal regime one is allowed to linearize the diode behavior. Still, the series resistance resulting from these small-signal quantities equals the series resistance obtained from the two-light-intensities method (also called “double illumination method”) [1, 3, 4] at that working point, $R_s = \Delta U_{\text{ext}} / \Delta I_{\text{ext}}$ (cf. Fig. 4) for larger (*i.e.*, usual) voltage and current differences, since the small-signal case is the limiting regime for decreasing differences of external voltage and external current strength.

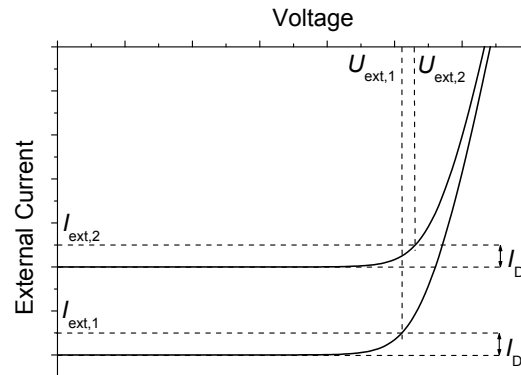


Fig. 4. Series resistance determination according to the two-light-level method (also known as double illumination method): From measuring two pairs of $I-U$ data corresponding to the same lumped dark diode current I_D , the series resistance corresponding to this lumped dark diode current is obtained as $R_s = \Delta U_{\text{ext}} / \Delta I_{\text{ext}}$.

The second basic step of the LR- R_s approach is to treat the voltage response in different orders of the (effective) emitter sheet resistivity ρ_{sh} and consider lateral series resistance effects as deviations from a perfect zero-resistance grid [15]. This is permitted since the emitter resistivity of standard industrial solar cells is rather low; that this approach is also physically justified comes out as a fundamental result. This basic idea – to make use of the fact that lateral voltage variations on real solar cells are typically small compared to the thermal voltage – is by far not new; it was already discussed and employed by Boone and van Doren [16] for what they called “properly designed” solar cells. It turns out that for “properly designed” solar cells (also called “economically reasonable” later on [17]) only the first order in ρ_{sh} is relevant (indicated by the index “1” in the following) [15].

Last but not least, the third and most far-reaching step of our theoretical approach is to obtain self-consistency with respect to current conservation in each order of the sheet resistivity (for the details see the appendix); only this brings in the variation of R_s along the $I-U$ characteristic. In the first order of ρ_{sh} and for the order-specific current-conservation-based self-consistency, the distributed part of the series resistance is [cf. Eq. (A-21) in the appendix]

$$\frac{1}{R_{s,1}^{\text{distr}}} = \frac{1}{R_{s,\infty}} + \frac{1}{R_D}. \quad (5)$$

Therefore, in the relevant voltage range this model predicts a slope of $g = 1$ [compare Eq. (5) with Eq. (3)] for the linear dependence of $1/R_s^{\text{distr}}$ on $1/R_D$.

From Eq. (5) one can understand the reason for the variation of R_s along the $I-U$ characteristic in a very simple way: This equation represents a parallel arrangement of two resistors, $R_{s,\infty}$ and R_D . At low voltages, when the lumped diode current is small and therefore the lumped effective diode resistance R_D is high [cf. Eq. (2)], one has that $R_s^{\text{distr}} \approx R_{s,\infty}$. However, for higher voltages where the lumped diode current starts to increase significantly, R_s^{distr} becomes smaller – because the diodes shorten some of the current so that the average lateral distance for current flow is reduced. This also explains which parts of the series resistance are distributed and which are non-distributed: All lateral paths that can be bypassed via the p-n junction are distributed, and the rest (as, e.g., the contact resistance or the resistance of the metallic grid) is not.

4. Results and discussion

In the previous works [11, 12], the present experimentally determined R_s data were interpreted in terms of a model based on theoretical results taken from Ref. [9]. Although meanwhile it was shown that the latter in some cases may lead to unphysical results [6], here we re-use the total series resistance value specified in [11, 12] for the

lowest injection, since in this regime the possible error is negligible. These total R_s values (which equal $R_s^{\text{nondistr}} + R_{s,\infty}$ since, at low injection, $R_D \rightarrow \infty$) are 3.94 m Ω for cell A and 4.42 m Ω for cell B. The LR- R_s model curves are obtained by imposing $g = 1$ and varying the non-distributed part that is subtracted from the total value, thereby also fixing the $R_{s,\infty}$ value, until a good match between the measured and the model data in Figs. 1(b) and 2(b) is obtained.

This way, the LR- R_s model curves for cell A, shown in red in Fig. 1, are obtained with $R_{s,\infty} = 1.95$ m Ω and $R_s^{\text{nondistr}} = 1.99$ m Ω , and for cell B the values are $R_{s,\infty} = 2.45$ m Ω and $R_s^{\text{nondistr}} = 1.97$ m Ω . That for each cell these numbers are quite similar, matches perfectly to observations made over many years on the share of the distributed and the non-distributed part of the total series resistance of “properly designed” solar cells investigated by the CELLO technique [17]: The distributed and non-distributed parts of R_s have practically always been found approximately equal in magnitude. This points to the series resistance of a solar cell being an efficient engineering solution: Any noticeable imbalance between these two parts of R_s would mean that either unnecessarily high losses or unnecessarily high effort (“over-engineering”) were involved.

Finally, we want to make two remarks about the problems related to the theoretical work of Araújo *et al.* [9] that go beyond the one already noted in Ref. [6]. In their work [9], current and voltage distribution in a one-dimensional geometry are determined as general as possible, and both the analytical and numerical results are accurate. However, then they derive an effective series resistance by assuming R_s in the standard one-diode model to be *external-current-dependent*, $R_s(I_{\text{ext}})$, which introduces a fundamental systematic error. This can be seen from their statement accompanying their Eq. (18) defining the current-dependent series resistance: “This common [...] definition of $R_s(I_{\text{ext}})$ permits us to represent the solar cell by an equivalent electrical circuit formed by an intrinsic diode and a lumped resistor in series.” Unfortunately, this is not true in general. In fact, just the opposite is correct: Only if one knows already that the *whole* solar cell can be described, on average, by the *same* values for the local series resistance and the local diode properties, then such an equivalent circuit may be used as a physically justified approximation for the whole solar cell, and then also their Eq. (18) equation holds. However, as soon as there are significant lateral inhomogeneities, this approximation becomes invalid, since then it is not the *whole* solar cell anymore for which the very same values are locally appropriate on average. And indeed, there are cases in which such inhomogeneities do occur (*e.g.*, under certain loading conditions), as has been discussed by Araújo *et al.* in detail for the phenomenon of current crowding.

However, even if there are no inhomogeneities that hinder the usage of an equivalent circuit, it is not advisable to use its relevant equation to introduce a lumped series resistance. This is so because from this equation one obtains an expression for R_s which makes it a function of many parameters, namely $R_s(I_{\text{ext}}, U_{\text{ext}}, I_{\text{ph}}, I_{01}, n_1)$. Nevertheless, as we have seen from the LR- R_s model, all these dependencies are irrelevant, since the only relevant one is the dependence on the dark diode current, *i.e.* $R_s(I_D)$ – independent of the strength or the flow direction of the other currents [6].

5. Summary and conclusions

For the first time, the LR- R_s model (originally developed for luminescence and CELLO measurements) has been successfully applied to injection-dependent series resistance data obtained from I - U characteristics, leading to a physically meaningful interpretation of the series resistance behavior. This is a strong hint that the physical concepts underlying the LR- R_s model and its consequences (*e.g.*, the straightforward explanation of the variation of R_s along the I - U characteristic) are of general validity for “properly designed” (=“economically reasonable”) solar cells. (Note that the LR- R_s model relies on typical properties of such cells and is not thought to be generally applicable.) Further work is needed to determine the g values of different data sets, resulting from various measurement methods, solar cell types, and solar cell geometries.

The equivalent circuit belonging to the LR- R_s model is nearly as simple as the standard one from which it deviates only slightly, but it fully includes the variation of R_s along the I - U characteristic due to its partly distributed nature. Most importantly, it describes correctly the physical dependency behind this variation: In all cases, the lumped series resistance depends only on the lumped dark diode current I_D . Thus, it is important to perform all related series resistance measurements at a fixed I_D and repeat the measurements for different I_D .

Acknowledgements

The authors are much obliged to Dr. O. Breitenstein, Max Planck Institute of Microstructure Physics, Halle (Saale), Germany. J.-M. Wagner acknowledges financial support from the Chair of Functional Nanomaterials, Technical Faculty at the University of Kiel.

Appendix A. Details of the LR- R_s model (one-dimensional approximation)

Here we show how to obtain the lumped LR- R_s model expression for the distributed part of the series resistance, Eq. (5), from an effective one-dimensional description of the full solar cell; it turns out that this simple description can provide sufficient information about the lateral voltage distribution to reasonably describe the lumped R_s effects.

A.1. Basic approximations

Let $x = 0$ be the center between two busbars of length l , located at $x = \pm b$ and running in y direction. From local measurements it is found (cf. [11] and references therein) that the voltage variation on the front surface of the solar cell is largest in x direction, and the variations in y direction are much smaller. This means that also the current distribution is mainly determined by the voltage variation in x direction. Accordingly, we introduce an effective one-dimensional description of the full two-dimensional voltage distribution of the solar cell by averaging all extensive solar cell properties (local photocurrent I_{ph} , local dark saturation current I_{01}) and the series resistances (emitter sheet resistance) along the y direction. For solar cells made from multicrystalline silicon (mc-Si) that do not show a spatial correlation of local series resistance and local diode properties (*i.e.*, for a sufficiently random variation of local diode properties [18]), this results in laterally homogeneous effective diode properties; then, for any given working point, in this effective 1D description R_D and the photocurrent are laterally constant. Due to this averaging in y -direction, the emitter is described by an effective (*i.e.*, including the influence of the grid fingers) sheet resistivity $\rho_{sh,eff}$.

The lumped currents I_{ext} (external current), I_{ph} (photocurrent), and I_D (dark diode current), the latter two being taken as positive quantities, fulfill the conservation relation $I_{ext} = I_D - I_{ph}$. The local vertical current density J_z at the p–n junction is given by $J_z(x) = J_D(x) - J_{ph}$. In the following, we employ a general notation principle: an overbar indicates all quantities referring directly to the solar cell's working point under investigation, while a tilde indicates all small variational quantities (deviations from this working point). The voltage distribution between the busbars is given by a function $\bar{U}(x)$. For the series resistance determination we consider the small additional voltage $\tilde{U}(x)$, *i.e.* we consider the full voltage $U(x) = \bar{U}(x) + \tilde{U}(x)$ (analogously for all other quantities). For symmetry reasons, the calculation is carried out for $x = 0 \dots b$ only; the transfer to the full situation is easy. As an approximation, we refer to the solar cell's working point by a lumped, area-related small-signal diode conductivity K (originally introduced in [14]), which is related to the current–voltage characteristic of an ideal diode (*i.e.*, without any series resistance involved) by

$$K := \frac{1}{A} \left. \frac{d\bar{I}_D}{dU} \right|_{\bar{U}_D}, \quad (\text{A-1})$$

with the active area $A = bl$ and I_D referring to this area. As discussed above, we describe the change in the local dark current density by $\tilde{J}_D(x) = K\tilde{U}(x)$ with a laterally homogeneous value of K , which is related to R_D by $K = G_D / A = 1 / (R_D A)$; cf. Eq. (2). Thus, the small-signal part of the vertical current density is given by $\tilde{J}_z(x) = K\tilde{U}(x) - \tilde{J}_{ph}$. To eliminate the contribution due to the photocurrent variation, we use the substitution

$$\tilde{U}(x) = U^*(x) + \tilde{J}_{ph} / K \quad (\text{A-2})$$

(*i.e.*, the homogeneous small-signal photocurrent just leads to a homogeneous offset in the small-signal voltage) and arrive at the linearized expression for the diode's and the photocurrent's deviations from the working point:

$$\tilde{J}_z(x) = KU^*(x). \quad (\text{A-3})$$

We now specify the basic differential equation governing the lateral voltage distribution, which is the standard Poisson equation for the 1D geometry in the linear-response approximation. The following current conservation relation holds for the small-signal lateral emitter sheet current: Since any current leaving the emitter [cf. Eq. (A-3)] comes from the external contact (which here is the busbar) at $x = b$ and flows in opposite direction to the x -axis (therefore the minus sign in the following equation), one has:

$$\tilde{I}_{\text{lat}}(x) = -l \int_0^x KU^*(x') dx'. \quad (\text{A-4})$$

The busbar length l appears as a factor because of the homogeneity in y -direction present in this model. From Ohm's law for the small-signal lateral sheet current density,

$$\frac{dU^*}{dx}(x) = -\rho_{\text{sh,eff}} \frac{\tilde{I}_{\text{lat}}(x)}{l}, \quad (\text{A-5})$$

one therefore has (since K is constant)

$$\frac{dU^*}{dx}(x) = \rho_{\text{sh,eff}} K \int_0^x U^*(x') dx'. \quad (\text{A-6})$$

From a further x -derivative, one obtains the basic differential equation for the linearized 1D case. For its solutions, the following boundary conditions are relevant: The external boundary condition, $\tilde{I}_{\text{lat}}(b) = -\tilde{I}_{\text{ext}}$ (as an external current, \tilde{I}_{ext} is taken as positive when flowing into the solar cell, but internally it flows in opposite direction to the x -axis, therefore the minus sign), expresses that at the busbar at $x = b$ the lateral current equals the external current:

$$\tilde{I}_{\text{ext}} = lK \int_0^b U^*(x') dx'. \quad (\text{A-7})$$

The internal boundary condition obviously is $\tilde{I}_{\text{lat}}(0) = 0$, which by Eq. (A-5) gives $\frac{dU^*}{dx}(0) = 0$.

A.2. Small-signal lumped series resistance determination

For small differences in external voltage and external current, the lumped series resistance according to the two-light-intensities method, $R_s = \Delta U_{\text{ext}} / \Delta I_{\text{ext}}$ (cf. Fig. 4), obviously corresponds for our small-signal formalism to

$$R_s = \tilde{U}_{\text{ext}} / \tilde{I}_{\text{ext}} \quad (\text{A-8})$$

for constant I_D , i.e., for $\tilde{I}_D = 0$. This requirement enforces a certain dependence between \tilde{U}_{ext} and \tilde{I}_{ext} , which will now be derived. According to the substitution defining $U^*(x)$, Eq. (A-2), we have that

$$\tilde{U}_{\text{ext}} = \tilde{U}(b) = U^*(b) + \tilde{J}_{\text{ph}} / K. \quad (\text{A-9})$$

We define the auxiliary function [that follows from the solution of Eq. (A-6)]

$$R(x) := U^*(x) / \tilde{I}_{\text{ext}}, \quad (\text{A-10})$$

so with $\tilde{J}_{\text{ph}} = \tilde{I}_{\text{ph}} / A$ and $(KA)^{-1} = R_D$, Eq. (A-9) becomes

$$\tilde{U}_{\text{ext}} = R(b) \tilde{I}_{\text{ext}} + R_D \tilde{I}_{\text{ph}}. \quad (\text{A-11})$$

This shows how, in general, a change in the external small-signal voltage is related to independent values of the small-signal currents \tilde{I}_{ext} and \tilde{I}_{ph} . For the lumped series resistance determination according to Eq. (A-8), however, $\tilde{I}_{\text{D}} = 0$ is mandatory, so there is no such independence. Instead, one obviously has $0 = \tilde{I}_{\text{D}} = \tilde{I}_{\text{ext}} + \tilde{I}_{\text{ph}}$, so that

$$\tilde{I}_{\text{ext}} = -\tilde{I}_{\text{ph}}. \tag{A-12}$$

For the series resistance determination according to the two-light-intensities method any variation of the photocurrent must exactly be compensated by a related change in the external current to keep the diode current constant. Inserting this into Eq. (A-11), we have from the fundamental small-signal series resistance definition, Eq. (A-8), that

$$R_s = R(b) - R_D. \tag{A-13}$$

A.3. Self-consistent analytical solution in different orders of the effective sheet resistivity

In zeroth order in $\rho_{\text{sh,eff}}$ (i.e., for vanishing $\rho_{\text{sh,eff}}$), it follows from Ohm’s law, Eq. (A-5), that the potential is constant; let this constant be c_0 . It follows from current conservation, Eq. (A-7), that $c_0 = R_D \tilde{I}_{\text{ext}} =: U_0^*$, and according to Eq. (A-10), $R_0 := U_0^* / \tilde{I}_{\text{ext}} = R_D$, so $R_{s,0} = 0$. From Eqs. (A-4) and (A-1) it follows that

$$\tilde{I}_{\text{lat},0} = -lKR_D \tilde{I}_{\text{ext}} x = -\tilde{I}_{\text{ext}} x/b. \tag{A-14}$$

The solutions in higher orders in the sheet resistivity are determined iteratively. This is done via Eq. (A-6) by inserting an n th order solution for $U^*(x)$ (containing a normalization factor that is to be determined) on its right-hand side, and due to the explicit factor $\rho_{\text{sh,eff}}$, the left-hand side of Eq. (A-6) provides the $(n+1)$ th order solution.

For the first order in $\rho_{\text{sh,eff}}$, it follows by using the constant c_1 for $U^*(x)$ on the right-hand side of Eq. (A-6) that

$$\frac{dU_1^*}{dx} = \rho_{\text{sh,eff}} K c_1 x, \tag{A-15}$$

which for the potential U_1^* itself (zeroth and first order in $\rho_{\text{sh,eff}}$) yields

$$U_1^*(x) = c_1 (1 + \frac{1}{2} \rho_{\text{sh,eff}} K x^2). \tag{A-16}$$

The boundary condition at $x = b$ (ensuring current conservation) can be expressed as $\frac{dU_1^*}{dx}(b) = \frac{\rho_{\text{sh,eff}} \tilde{I}_{\text{ext}}}{l}$ [cf. Eq. (A-5)], and using this on the left-hand side of Eq. (A-6) with Eq. (A-16) inserted on the right-hand side one has that

$$\tilde{I}_{\text{ext}} = lKc_1 (b + \frac{1}{6} \rho_{\text{sh,eff}} K b^3), \tag{A-17}$$

yielding

$$c_1 = \frac{R_D \tilde{I}_{\text{ext}}}{1 + \frac{1}{6} \rho_{\text{sh,eff}} K b^2}; \tag{A-18}$$

therefore

$$U_1^*(x) = \tilde{I}_{\text{ext}} \frac{R_D + \frac{1}{2} \rho_{\text{sh,eff}} x^2 / (bl)}{1 + \frac{1}{6} R_D^{-1} \rho_{\text{sh,eff}} b/l}. \tag{A-19}$$

Despite the appearance of $\rho_{\text{sh,eff}}$ in the denominator of Eq. (A-19), this still represents the linear order in $\rho_{\text{sh,eff}}$

since in the denominator, its influence depends on R_D , and for low diode voltages, $R_D^{-1} \rightarrow 0$, and then only the numerator remains. In this order of $\rho_{sh,eff}$, the small-signal expression for the lumped series resistance according to the two-light-intensities method, Eq. (A-13), leads to

$$R_{s,1} = R_1(b) - R_D = \frac{\frac{1}{3} R_D \rho_{sh,eff} K b^2}{1 + \frac{1}{6} \rho_{sh,eff} K b^2} = \frac{\frac{1}{3} \rho_{sh,eff} b/l}{1 + \frac{1}{6} \rho_{sh,eff} b/(l R_D)}. \quad (A-20)$$

However, because it results from a distributed network, one has that R_s is not constant but varies along the $I-U$ curve: Taking the inverse of Eq. (A-20) one has

$$\frac{1}{R_{s,1}} = \frac{1 + \frac{1}{6} \rho_{sh,eff} K b^2}{R_D \frac{1}{3} \rho_{sh,eff} K b^2} = \frac{1}{\frac{1}{3} \rho_{sh,eff} b/l} + \frac{1}{2 R_D} =: \frac{1}{R_{s,\infty}^{1D}} + \frac{1}{2 R_D}, \quad (A-21)$$

where $R_{s,\infty}^{1D} = \frac{1}{3} \rho_{sh,eff} b/l$ is the well-known expression for the effective series resistance contribution of the sheet resistivity for the 1D geometry; this expression was derived already in other works (cf., e.g., [15, 19]). Since at a busbar the situation is symmetric with respect to both of its sides, the relevant area is twice as large as considered so far, implying that diode resistance has half the value considered so far; thus, the factor of 2 cancels in Eq. (A-21), and also the value of $R_{s,\infty}^{1D}$ is halved (cf. Eq. (21) of [19]). Altogether, we end up with Eq. (5).

References

- [1] Wolf M, Rauschenbach H. Series resistance effects on solar cell measurements. *Advanced Energy Conversion* 1963;3:455–79.
- [2] Bhattacharya DK, Mansingh A, Swarup P. Dependence of series resistance on operating current in p-n junction solar cells. *Solar Cells* 1986;18:153–62.
- [3] Altermatt PP, Heiser G, Aberle AG, Wang A, Zhao J, Robinson SJ, Bowden S, Green MA. Spatially resolved analysis and minimization of resistive losses in high-efficiency Si solar cells. *Progress in Photovoltaics: Research and Applications* 1996;4:399–414.
- [4] Fong KC, McIntosh KR, Blakers AW. Accurate series resistance measurement of solar cells. *Progress in Photovoltaics: Research and Applications* 2013;21:490–9.
- [5] Turek M. Current and illumination dependent series resistance of solar cells. *Journal of Applied Physics* 2014;115:144503.
- [6] Wagner J-M, Schütt A, Carstensen J, Adelung R. Linear-response description of the series resistance of large-area silicon solar cells: Resolving the difference between dark and illuminated behavior. *Energy Procedia* 2016;92:255–64.
- [7] Rajkanan K, Shewchun J. A better approach to the evaluation of the series resistance of solar cells. *Solid-State Electronics* 1979;22:193–7.
- [8] Dhariwal SR, Mittal S, Mathur RK. Theory for voltage dependent series resistance in silicon solar cells. *Solid-State Electronics* 1984;27:267–73.
- [9] Araújo GL, Cuevas A, Ruiz JM. The effect of distributed series resistance on the dark and illuminated current voltage characteristics of solar cells. *IEEE Transactions on Electron Devices* 1986;33:391–401.
- [10] Vishnoi A, Gopal R, Dwivedi R, Srivastava SK. Distributed parameter analysis of dark $I-V$ characteristics of the solar cell: estimation of equivalent lumped series resistance and diode quality factor. *IEE Proceedings G (Circuits, Devices and Systems)* 1993;140:155–64.
- [11] Breitenstein O, Rißland S. A two-diode model regarding the distributed series resistance. *Solar Energy Materials & Solar Cells* 2013; 110:77–86.
- [12] Rißland S, Breitenstein O. Considering the distributed series resistance in a two-diode model. *Energy Procedia* 2013;38:167–75.
- [13] Wagner J-M, Hoppe M, Schütt A, Carstensen J, Föll H. Injection-level dependent series resistance: Comparison of CELLO and photoluminescence-based measurements. *Energy Procedia* 2013;38:199–208.
- [14] Carstensen J, Schütt A, Föll H. CELLO local solar cell resistance maps: Modeling of data and correlation to solar cell efficiency. In: *Proceedings of the 22nd European Photovoltaic Energy Conference and Exhibition, Milan, Italy (2007)*, contribution 1CV.1.34.
- [15] Nielsen LD. Distributed series resistance effects in solar cells. *IEEE Transactions on Electron Devices* 1982;29:821–7.
- [16] Boone JL, van Doren TP. Solar-cell design based on a distributed diode analysis. *IEEE Transactions on Electron Devices* 1978;25:767–71.
- [17] Carstensen J, Schütt A, Föll H. Modelling of the distributed grid resistance: verification by CELLO measurements and generalization to other resistance mapping tools. In: *Proceedings of the 23rd European Photovoltaic Energy Conference and Exhibition, Valencia, Spain (2008)*, contribution 1CV.1.38.
- [18] Carstensen J, Wagner J-M, Schütt A, Föll H. Relation between local and global $I-U$ characteristics: restrictions for and by series resistance averaging. In: *Proc. of the 29th European Photovoltaic Energy Conference, Amsterdam, The Netherlands (2014)*, contribution 2BV.8.21.
- [19] Wyeth NC. Sheet resistance component of series resistance in a solar cell as a function of grid geometry. *Solid-State Electronics* 1977; 20:629–34.